

The chemical composition of carbon stars. The R-type stars

O. Zamora¹, C. Abia¹, B. Plez², I. Domínguez¹, and S. Cristallo^{1,3}

¹ Departamento de Física Teórica y del Cosmos, Universidad de Granada, 18071 Granada, Spain
e-mail: zamora@ugr.es

² GRAAL, Université Montpellier II, CNRS, 34095 Montpellier Cedex 5, France

³ INAF, Osservatorio Astronomico di Collurania, 64100 Teramo, Italy

ABSTRACT

Aims. The aim of this work is to shed some light on the problem of the formation of carbon stars of R-type from a detailed study of their chemical composition.

Methods. We use high-resolution and high signal-to-noise optical spectra of 23 R-type stars (both early- and late-types) selected from the Hipparcos catalogue. The chemical analysis is made using spectral synthesis in LTE and state-of-the-art carbon-rich spherical model atmospheres. We derive their CNO content (including the $^{12}\text{C}/^{13}\text{C}$ ratio), average metallicity, lithium, and light (Sr, Y, Zr) and heavy (Ba, La, Nd, Sm) *s*-element abundances. The observed properties of the stars (galactic distribution, kinematics, binarity, photometry and luminosity) are also discussed.

Results. Our analysis shows that late-R stars are carbon stars with identical chemical and observational characteristics than the normal (N-type) AGB carbon stars. In fact, the *s*-element abundance pattern derived can be reproduced by low-mass AGB nucleosynthesis models where the $^{13}\text{C}(\alpha, n)^{16}\text{O}$ reaction is the main neutron donor. We confirm the results of the sole previous abundance analysis of early-R stars by Dominy (1984), namely: they are carbon stars with near solar metallicity showing enhanced nitrogen, low $^{12}\text{C}/^{13}\text{C}$ ratios and no *s*-element enhancements. In addition, we have found that early-R stars have Li abundances larger than expected for post RGB tip giants. We also find that a significant number ($\sim 40\%$) of the early-R stars in our sample are wrongly classified, being probably classical CH stars and normal K giants.

Conclusions. On the basis of the chemical analysis, we confirm the previous suggestion that late-R stars are just misclassified N-type carbon stars in the AGB phase of evolution. Their photometric, kinematic, variability and luminosity properties are also compatible with this. In consequence, we suggest that the number of true R stars is considerably lower than previously believed. This alleviates the problem of considering R stars as a frequent stage in the evolution of low-mass stars. We briefly discuss the different scenarios proposed for the formation of early-R stars. The mixing of carbon during an anomalous He-flash is favoured, although no physical mechanism able to trigger that mixing has been found yet. The origin of these stars still remains a mystery.

Key words. stars: abundances – stars: chemically peculiar – stars: carbon – stars: AGB and post-AGB – stars: evolution

1. Introduction

Carbon stars are easily recognisable by the presence of absorption bands of C_2 and CN at near visual wavelengths and are chemically characterised by $\text{C}/\text{O} > 1$ in their envelope. The Henry Draper classification divided carbon stars into the N and R groups on the basis of their spectral features. The N or normal carbon stars, show a very strong depression in the spectrum at $\lambda < 4500 \text{ \AA}$, while the R stars seem to be warmer and the blue/violet region of the spectrum is usually accessible to observations. Shane (1928) split the R class into R0 to R8, where R0-4 (hot-early-R stars) are warmer and equivalent to the K-type giants, and R5-8 (cool-late-R stars) are equivalent to M stars. Since $\text{C}/\text{O} < 1$ almost everywhere in the Universe, the carbon excess must be a result of stellar nucleosynthesis within the star itself or in a binary companion. The N stars are understood in the former scenario: they are luminous, cool stars with alternate H- and He-burning shells, that owe their carbon enhancement to the mixing triggered by the third dredge-up during the asymptotic giant branch (AGB) phase in the evolution of low-mass ($< 3 M_{\odot}$) stars (e.g. Iben & Renzini 1983). Other carbon stars like the classical CH-type are observed to be members of binary systems and their

chemical peculiarities can be explained by the second scenario as a consequence of mass transfer (Han et al. 1995).

The R stars seem to be very common among the giant carbon stars, accounting 10 times more than the N stars (Blanco 1965). According to the general catalogue of carbon stars (Stephenson 1973), R-type stars may amount to $\sim 30\%$ of all the carbon stars. Bergeat et al. (2002a) suggested that this fraction might be even larger. This figure is very important since they may represent a stage of evolution that is available to an appreciable fraction of stars, and are not the result of anomalous initial conditions or statistically unlikely events. Further, their velocity dispersion and position in the Galaxy indicates that early-R stars are members of the galactic thick disk while late-R show kinematic properties rather similar to the thin disk stellar population (e.g. Sanford 1944; Eggen 1972; Bergeat et al. 2002b). The luminosities of R stars (at least the early-R) are known to be too low to be shell helium burning stars (e.g. Scalo 1976). In this sense, a fundamental step was made by Knapp et al. (2001) whose re-processing of the Hipparcos data (Perryman & ESA 1997), located R stars in the H-R diagram at the same place than the red clump giants and concluded that they were He-core burning stars or post helium core stars. Another fundamental property of these stars is that no

R star has been found so far in a binary system (McClure 1997), a statistically unlikely result.

The only chemical analysis by Dominy (1984) showed that early-R stars have near solar metallicity, low (< 10) $^{12}\text{C}/^{13}\text{C}$ ratios, moderate nitrogen excess and no *s*-element enhancements. No chemical analysis of late-R stars exists up to date. This finding for early-R stars is also in sharp contrast with that found in N-type carbon stars (Abia et al. 2002). So, the problem is how a *single* giant star not luminous enough to be on the AGB phase can present a $\text{C}/\text{O} > 1$ at the surface. The favoured hypothesis so far is that the carbon produced during the He-flash is mixed in some way to the surface. However, standard one-dimensional He-flash models do not predict the mixing of carbon-rich material from the core to the stellar envelope (Härm & Schwarzschild 1966). A lively discussion about this subject was held following the first suggestion of mixing at the He-flash proposed by Schwarzschild & Härm (1962). Models in which rotation was parametrised (Mengel & Gross 1976) lead to off-center He-ignition but not to conditions favouring mixing. On the other hand, models in which the location of the He-ignition was ad hoc moved to the outer part of the He-core (Paczynski & Tremaine 1977) produced the desired mixing. The general conclusion being (Despain 1982) that hydrostatic models do not produce mixing at the He-flash. The situation is different for $Z=0$ models (Fujimoto et al. 1990; Hollowell et al. 1990) but in this case the mixing is directly linked to the lack of CNO elements in the H-shell and it can not be extrapolated to more metal-rich models¹. Recently, two- and three-dimensional hydrodynamic simulations of the core He-flash in Population I stars have been performed (Lattanzio et al. 2006; Mocák et al. 2008a,b; Mocák 2009). None of these simulations lead to substantial differences with respect to the hydrostatic case. Thus, no physical mechanism able to trigger the required mixing of carbon during the He-flash in single stars has been found up to date. Binary star mergers have been invoked to induce such mixing. This, by passing, might explain why no R star is found to be binary. Izzard et al. (2007) investigate statistically possible channels for early-R star formation by a binary merger process. They found many possible evolutionary channels, the most common of which is the merger of a He white dwarf with a hydrogen-burning red giant branch star during a common envelope phase. However, it is far from clear if such a merger might lead to the mixing of carbon to the surface during the He-flash (Zamora 2009).

In order to shed light on the problem of the origin of these stars, we present here a detailed chemical analysis of late- and early-R stars using high quality spectra. This is a further step in the study of the chemical composition of field giant carbon stars in the Galaxy. In Paper I (Abia & Isern 2000) we studied J-type stars and in Papers II and III (Abia et al. 2001, 2002) the N-type stars. In the next section we describe the main characteristics of the sample stars and the observations. Sect. 3 describes the determination of the stellar parameters and chemical analysis, and Sect. 4 discusses the results and draws some conclusions.

2. The data

2.1. Observations

We selected 23 galactic R-type stars from the sample of carbon stars compiled by Knapp et al. (2001) with measured para-

llaxes according to Hipparcos (Perryman & ESA 1997). The stars were observed with the 2.2 m telescope at CAHA observatory (Spain) during March 2003 and July/August 2004. Spectra were obtained using the FOCES echelle spectrograph (Pfeiffer et al. 1998). The spectra cover the wavelength region from $\lambda \sim 4000 - 10700 \text{ \AA}$ in 90 orders with full spectral coverage, a resolving power of $R \sim 40000$ in most of the spectra except those obtained in the last period of observation ($R \sim 20000$), because of the 2×2 CCD binning made to increase the signal-to-noise ratio in the spectrum of the fainter stars. The typical S/N ratio reached in the spectra was larger than 100 in the red orders and lower than this value below $\lambda \sim 5000 \text{ \AA}$. In fact, in some stars the blue orders were not useful for the abundance analysis.

The spectra were reduced using the *echelle* task within the IRAF package following the standard procedure. When several images of the same object were obtained, they were reduced independently and finally added using the IRAF task *combine*. The wavelength calibration was always better than 0.03 \AA . Finally, the individual spectral orders were normalised to a pseudo-continuum by joining the maximum flux points and, in some cases, corrected with the help of the synthetic spectra (see details of the method in Paper I). We estimate an uncertainty in the continuum location of less than a 5%, although it may be larger for the spectral orders severely affected by molecular bands, particularly in late-R stars.

2.2. Spectral classification

One of the most serious problems when dealing with carbon stars in general is their ascription to one or another spectral type. This is because the spectral classification is done frequently by using low resolution spectra, which does not permit the detection of relevant atomic lines due to blends with molecular bands (e.g. Cannon & Pickering 1918; Shane 1928; Keenan & Morgan 1941; Vandervort 1958; Keenan 1993; Barnbaum et al. 1996). In this sense, studies on early-R stars are frequently contaminated with CH-type stars, whose spectral distribution is very similar (see e.g. Wallerstein & Knapp 1998). In fact, the most effective way of distinguishing between these two spectral types is to compare the intensity of some metallic lines (less prominent in CH-type stars) and, mainly, the intensity of *s*-element lines which are well known to be enhanced in CH-type stars (Keenan 1993; Abia et al. 2003; Goswami 2005). An additional problem concerns the derivation of the temperature subtype. In general the intensity of C-bearing molecular bands in carbon stars depends not only on the effective temperature but also on the actual C/O ratio in the atmosphere. In the case of early-R stars this introduces an extra uncertainty in the assignation of the temperature subtype compared with normal (O-rich) G- and K-type stars of similar effective temperature. For the late-R stars, there is no tight correlation between the spectral distribution and effective temperature due to the presence of very intense molecular absorptions, similar to N-type stars (Keenan 1993). Table 1 shows the spectral classification of our stars from different sources in the literature. It is evident that many stars have been classified in very different ways because of the problems cited above.

This confusion in the spectral classification of many R-type stars has motivated the use of others criteria such as the photometric one. For instance, Knapp et al. (2001) use the $(V - K)$ colour index to distinguish between early and late-type R stars according whether $(V - K)_0 < 4$ or $(V - K)_0 > 4$, respectively. Since many colour indexes might be affected by the variability of the star (at least for the late-R) and also by the presence of strong

¹ We remind that from the analysis by Dominy (1984), R stars have $[\text{Fe}/\text{H}] \sim 0.0$. In this paper we adopt the usual notation $[\text{X}/\text{H}] = \log \text{N}(\text{X})/\text{N}(\text{H}) - \log \text{N}(\text{X})/\text{N}(\text{H})_{\odot}$, where $\log \text{N}(\text{H}) \equiv 12$ is the hydrogen abundance by number.

Table 1. Log of the observations and spectral classification.

HIP	Name			Var. Type	Date (*)	Exp. (s)	Spectral Type
	BD	HD	GCVS				
35 810	-03°1873	57 884	V758 Mon	Lb	1	3000	N (9), R8 (12)
36 623	+24°1686	59 643	NQ Gem	SR	1	3600	R9 (12), R6 (9), R8 (15)
39 118	-	-	-	-	1	3600	R2 (15)
44 812	-	78 278	-	-	1	3600	R6 (9), R5 (15)
53 832	+41°2150	-	-	-	1	3600	R0 (15), CH-like (16), CH (2)
58 786	+71°600	-	-	-	1	3600	R2 (15), CH-like (17), CH (2)
62 401	+04°2651a	111 166	RU Vir	Mira	1	3600	R3 (9), R3 (15)
62 944	-	112 127	-	-	1	2400	K0 (13), K1 (14), K2 (11, 8, 10), K3 (7), R3 (1)
69 089	-	123 821	-	-	1	3600	G9 (7), G8 (11), R2 (4), R2 (1)
74 826	+30°2637	-	-	-	1	2700	R0 (12)
82 184	+23°2998	-	-	-	3	3600	R0 (15), R2 (1)
84 266	+42°2811	156 074	-	-	2	2400	R0 (11, 17), R1 (5), R2 (1)
85 750	+02°3336	-	-	-	3	3600	R2 (15), CH-like (17), N5 (4), N4 (1)
86 927	+17°3325	-	-	-	2	3000	R0 (12)
87 603	-	163 838	-	-	3	5400	R3 (9), R5 (15)
88 887	+09°3576	166 097	-	-	2	3600	R4 (9), R5 (15)
91 929	-13°5083	173 138	RV Sct	Lb	3	3600	R3 (9), R3 (15), R4 (1)
94 049	-17°5492	178 316	-	-	3	5400	R4 (12), R2 (9)
95 422	-	-	-	-	3	5400	R5 (15)
98 223	-00°3883	188 934	-	-	3	7200	R8 (12), R4 (9)
108 205	+49°3673	208 512	LW Cyg	Lb	3	4200	R3 (9), R2 (15), R8 (3)
109 158	-	-	CT Lac	SRa	3	5400	R (6), N8 (3)
113 150	-	216 649	-	-	3	3300	R3 (9), R5 (15)

* (1) 2003 March 12-13; (2) 2003 August 9-10; (3) 2004 July 1-4.

References for the spectral types:

1: Barnbaum et al. (1996); 2: Bartkevicius (1996); 3: Egilitis et al. (2003); 4: Keenan (1993); 5: Keenan & Morgan (1941); 6: Lee & Bartlett (1944); 7: McClure (1970); 8: Morgan & Keenan (1973); 9: Sanford (1944); 10: Schild (1973); 11: Schmitt (1971); 12: Shane (1928); 13: Stock & Weihau (1956); 14: Uppgren (1962); 15: Vandervort (1958); 16: Yamashita (1972); 17: Yamashita (1975).

The following stars show evidence of binarity:

HIP 36 623 (Carquillat & Prieur 2008), HIP 109 158 (Makarov & Kaplan 2005), HIP 53 832 (Platais et al. 2003) and HIP 85 750 (McClure 1997).

molecular absorptions, we simply adopt here the criterion based on the effective temperature estimated in the chemical analysis (see Sect. 3). We will see, that an effective temperature threshold of ~ 3600 K seems to be a good criterion to distinguish between early- and late-R stars. This will lead to a spectral classification in agreement with the Knapp et al. (2001)'s criterion above, and with other characteristics that differentiate the two subtypes of R stars.

2.3. Distribution in the Galaxy and kinematics

That the R stars are galactic disk objects was recognised by Eggen (1972). Bergeat et al. (2002b) calculated the space density in the galactic plane of early-R stars and found that it is a factor ~ 16 lower than for N stars; in fact, on average they are three times further from the galactic plane. Despite the small sample studied here, we reach the same conclusion: our early-R stars are located at large galactic latitudes, $|b| \geq 30^\circ$. The distribution of the late-R stars is however, almost identical to that of the N-type stars (e.g. Claussen et al. 1987): they are very close to the galactic plane. These differences in the galactic distribution of R stars were already known (e.g. Sanford 1944; Ishida 1960; Rybski 1972; Stephenson 1973; Barbaro & Dallaporta 1974) and are indicative of early-R stars belonging to the galactic thick disk while late-R stars belong to the thin disk. This of course implies a range for the masses and ages of the R stars: early-R stars must be of lower masses ($\leq 1 M_\odot$) and older than late-R stars.

Previous kinematics analyses performed by e.g. Dean (1972) and recently by Bergeat et al. (2002b) show that the velocity dispersion of R-stars are typically larger by a factor of ~ 2 than for N-type stars. Bergeat et al. (2002b) in particular, obtain $\sigma = 42 - 54$ km s $^{-1}$ in the direction of the galactic north pole for the stars belonging to their *hot carbon* group², where most of our early-R are included, and 23 km s $^{-1}$ typically for the *cool variable* group, which includes the late-type stars in our sample. This reinforce the conclusion that the differences between early- and late-type R stars are representative of two different stellar populations, as we already noted. According to this numbers, and applying a standard age-velocity relation (e.g. Wielen et al. 1992), an age of ~ 3 Gyr and ≥ 10 Gyr is obtained for late- and early-R stars, respectively.

2.4. Binarity

Table 1 indicates the stars with evidence of binarity obtained from radial velocity variations or other methods. These stars are HIP 53 832 and HIP 85 750, classified as early-R, and the late-R stars HIP 36 623 and HIP 109 158. It is important to note that these two early-R stars have been also classified as CH-

² Bergeat et al. (2002b) define 14 photometric groups in order to classify the carbon stars observed by Hipparcos into homogeneous classes. They define the *hot carbon* (HC) group which includes mostly early-R and CH-type stars, whereas the *cool variables* (CV) group includes N-type stars and a few late-R stars.

Table 2. Photometric data and luminosities

Star	<i>V</i>	<i>K</i>	<i>J</i> − <i>H</i>	<i>H</i> − <i>K</i>	<i>M</i> _{<i>K</i>0}	<i>M</i> _{bol}	Ref.
Late-R stars							
HIP 35 810	9.01	3.67	0.83	0.42	−6.84	−4.05	1
HIP 36 623	8.02	2.95	0.72	0.38	−7.23	−4.18	5
HIP 62 401	11.98	1.81	1.85	1.30	−7.48	−5.23	7
HIP 91 929	9.75	3.41	1.30	0.51	−7.25	−4.96	1
HIP 108 205	9.23	1.71	1.36	0.80	−8.57	−5.45	4, 1
HIP 109 158	10.12	2.57	1.21	0.75	−8.90	−5.65	5, 1
Early-R stars							
HIP 39 118*	10.41	7.23	0.79	0.25	−2.18	0.47	1
HIP 44 812	10.61	6.50	0.78	0.35	−4.73	−2.02	1
HIP 53 832	10.11	7.60	0.52	0.13	−2.83	−0.81	1
HIP 58 786	10.27	7.51	0.52	0.15	−3.06	−1.02	1
HIP 62 944*	6.91	4.16	0.55	0.10	−1.27	0.86	3
HIP 69 089*	8.68	6.40	0.46	0.12	−3.09	−1.24	1
HIP 74 826	9.78	7.39	0.48	0.12	−3.31	−1.38	1
HIP 82 184	9.10	6.46	0.57	0.12	−3.67	−1.04	1
HIP 84 266	7.60	5.11	0.30	0.23	−3.09	−0.87	5
HIP 85 750	9.42	5.15	0.82	0.24	−5.85	−3.25	2, 1
HIP 86 927	8.71	6.14	0.53	0.14	−1.69	0.22	2
HIP 87 603	10.72	7.92	0.55	0.18	−2.24	−0.02	1
HIP 88 887	9.78	5.13	0.84	0.36	−5.90	−3.14	1
HIP 94 049	10.39	7.39	0.55	0.19	−3.82	−1.97	1
HIP 95 422	11.01	6.74	0.75	0.26	−4.81	−2.57	1
HIP 98 223	9.36	5.15	0.78	0.31	−6.27	−3.78	6, 1
HIP 113 150	10.75	7.97	0.55	0.22	−3.45	−1.26	1

Non dereddened *VJHK* magnitudes.

References of photometry:

1: 2MASS Cutri et al. (2003); 2: Dominy et al. (1986); 3: Elias (1978); 4: Neugebauer & Leighton (1969); 5: Noguchi et al. (1981); 6: Mendoza & Johnson (1965); 7: Whitelock et al. (2000).

type stars, which are known to be all binaries. We will reach the same conclusion on the basis of their chemical composition (see Sect. 4.1). HIP 85 750 is a binary system whose orbital parameters were determined by McClure (1997). The late-R star HIP 36 623 is a symbiotic star detected by time-variations of the ultra-violet continuum due probably to the presence of a white dwarf companion (Johnson et al. 1988; Belczyński et al. 2000; Munari & Zwitter 2002). Recently, Carquillat & Prieur (2008) estimate that the components of the system have masses of 2.5 M_{\odot} and 0.6 M_{\odot} . On the other hand, HIP 109 158 appears in the catalogue of Hipparcos astrometric binaries with accelerated proper motions (Makarov & Kaplan 2005). For the remaining sample, there is no evidence of binarity (in agreement with the study by McClure 1997) or available study.

2.5. Photometry

Table 2 shows the available *VJHK* photometry taken from Knapp et al. (2001), the Hipparcos catalogue or from the 2MASS (*Two Micron All Sky Survey*) on-line data release (Cutri et al. 2003). Differences in the photometry found in the literature for a given star are typically below ~ 0.2 mag for the majority of early-R stars, but it can be higher for late-R stars due to their known photometric variability (see Table 1). All the photometric magnitudes were corrected from interstellar extinction using the A_J values derived by Bergeat et al. (2002a)

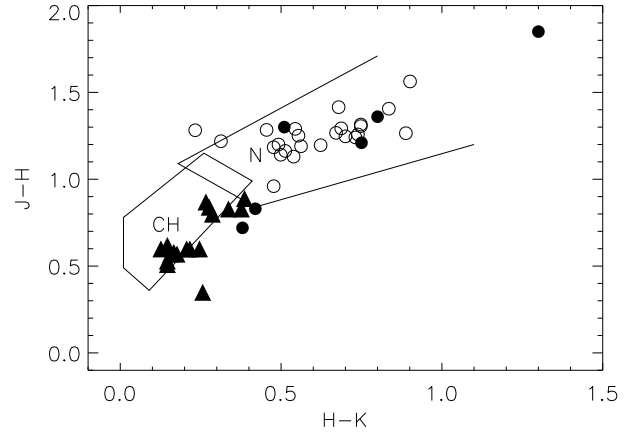


Fig. 1. Near infrared colour-colour diagram for the stars in this study. Triangles are early-R stars, filled circles late-R stars and empty circles the N-type stars from Abia et al. (2001). The regions typically populated by CH- and N-type stars are indicated (Totten et al. 2000).

and the relations by Cardelli et al. (1989). For the stars HIP 39 118, HIP 62 944 and HIP 69 089, not included in the Bergeat et al. (2002a) sample, we use the galactic interstellar extinction model by Arenou et al. (1992) and the parallaxes by Knapp et al. (2001). In Fig. 1 the position of our sample stars is plotted in the near infrared colour-colour diagram. We have marked with lines the regions usually occupied by CH- and N-type stars according to Totten et al. (2000). Some galactic carbon stars of N-type (Paper II) are included for comparison. It is clear from this figure that early-R stars occupy the same region as CH-type stars, while late-R stars are redder and are located mostly in the region of N-type carbon stars.

Another interesting photometric index is the $K - [12]^3$ colour, which is considered a tracer of the dust surrounding the star (Jorissen & Knapp 1998). The formation of circumstellar dust is considered a measure of the stellar mass-loss and in consequence might give an indication of the evolutionary status of a given star: stars with no mass-loss or very low rates have $K - [12] \leq 0.7$. Our early-R stars fulfil this criterion and do not present significant mass-loss. At contrary, most of our late-R stars show $K - [12] > 0.7$ and would correspond to stars with moderate mass-loss rates, 5×10^{-8} to $5 \times 10^{-7} M_{\odot} \text{ y}^{-1}$, the extreme case being HIP 62 401 ($K - [12] = 4.1$) having a considerably larger rate, $10^{-6} M_{\odot} \text{ y}^{-1}$ (the star in the upper right corner in Fig. 1). These numbers are similar to those estimated in normal AGB stars (see e.g. Busso et al. 2007).

2.6. Luminosity

As we mentioned above, the selected stars have all measured trigonometric parallaxes according to Hipparcos (Perryman & ESA 1997). However, Hipparcos parallaxes for giant stars resulted to be not very accurate. Knapp et al. (2001) reprocessed the original Hipparcos parallaxes by imposing the condition that they remained always greater than zero (see also Pourbaix & Jorissen 2000). In the sample of R

³ $[12] = -2.5 \log (F_{12}/28.3)$, where F_{12} is the IRAS flux density at 12 μm .

stars in Knapp et al. (2001) only 18 % of the stars have $\pi/\epsilon(\pi) > 2$, where π denotes the trigonometric parallax and $\epsilon(\pi)$ the associated error. Knapp et al. (2001) performed a re-reduction of the *Intermediate Astrometric Data* (IAD, van Leeuwen & Evans 1998) taking as parameter, in the χ^2 minimisation, the logarithm of the distance instead of the distance itself. In this way, the derived parallaxes are always greater than zero. The true parallaxes, i.e. the parallaxes free of all the possible biases (see e.g. Arenou & Luri 1999), were then estimated with a Monte-Carlo simulation by adopting different distributions for the abscissa residuals of the IAD (see also Pourbaix & Jorissen 2000). Following this procedure, these authors derived a true average absolute K -magnitude for the early-R stars: $M_{K_0} = -2 \pm 1$, similar to the value -1.61 ± 0.03 found by Alves (2000) for red clump giant stars near the Sun observed by Hipparcos. Another major study on the parallaxes of R stars was made by Bergeat et al. (2002a). These authors use the original Hipparcos parallaxes and correct them from all the observational biases (that may introduce an uncertainty up to ~ 0.4 mag in the estimation of the luminosity, see e.g. Bergeat et al. 2002a for further details), obtaining significantly different results. In fact, they find an average K -absolute magnitude of $M_{K_0} = -3.0$ for early-R stars. Correspondingly, they derive also bolometric magnitudes for R type stars $\sim 1 - 2$ mag brighter than those obtained by Knapp et al. (2001). We believe that the parallaxes by Bergeat et al. (2002a) are more accurate since the parallaxes by Knapp et al. (2001) might undergo a bias when $K \geq 8$, whose effect is to overestimate the M_K (see their Fig. 2). On the other hand, a new analysis of the Hipparcos data has been performed recently by van Leeuwen (2007). The absolute magnitudes computed with these new data for our stars (13 of them) are in general in good agreement with those derived by Bergeat et al. (2002a), with a maximum difference below 0.5 magnitudes. Therefore, we have adopted here the parallaxes derived by Bergeat et al. (2002a) to estimate the luminosity of our stars. For HIP 39 118, HIP 62 944 and HIP 69 089 (not included in the Bergeat et al. 2002a sample, as previously noted) we use instead Knapp et al. (2001) parallaxes.

Table 2 shows the absolute magnitude in the K band corrected for interstellar extinction (M_{K_0}). The corresponding absolute bolometric magnitudes (M_{bol}) according to Bergeat et al. (2002a) are also shown. For the stars HIP 39 118, HIP 62 944 and HIP 69 089 we used the bolometric correction in K by Costa & Frogel (1996). We note that the error in the derivation of M_{K_0} and M_{bol} can be as large as $\sim 1 - 1.5$ mag, and it is dominated by the uncertainty in the trigonometric parallaxes. Nevertheless, we have constructed the H-R diagram of the stars in the sample (see next section for details in the derivation of the T_{eff}). From Fig. 2 it is clear that the luminosities of late-R stars are close to the values expected for low-mass stars ($< 2 M_{\odot}$) in the AGB phase. In Fig. 2 is also drawn the minimum luminosity (dashed line at $M_{\text{bol}} \approx -4.5$) for a $1.4 M_{\odot}$ star to become a thermally-pulsing AGB carbon star according to Straniero et al. (2003). This luminosity limit is quite model dependent (metallicity, mass loss history, third dredge-up efficiency, treatment of the opacity in the envelope etc, see Straniero et al. 2003), but roughly indicates that late-R stars have luminosities compatible with the AGB values. At contrary, early-R stars are clearly below the expected luminosity in this phase.

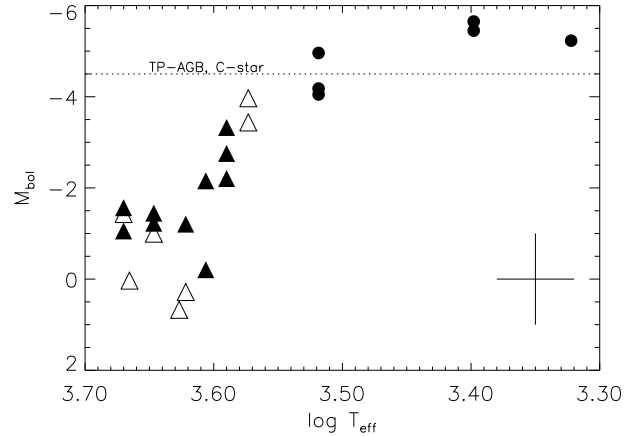


Fig. 2. H-R diagram for the sample stars. Solid triangles are early-R stars and circles late-R stars. Open triangles correspond to stars classified as early-R stars in the Hipparcos catalogue which have been reclassified here as K- or CH-type giants (see Sect. 4).

3. Atmospheric parameters and abundance calculations

We use the latest generation of MARCS spherically-symmetric model atmospheres for carbon stars (Gustafsson et al. 2008). In this new grid however, there is no a complete set of carbon enhanced models for $T_{\text{eff}} \geq 3500$ K. For stars with effective temperature larger than this value, we use MARCS C-rich models computed by one of us (B. Plez).

The estimation of the atmospheric parameters was made in a similar way to Papers II and III, and will be only briefly described here. We refer to these previous works for more details. We followed an iterative method that compares computed and observed spectra modifying T_{eff} , gravity, average metallicity and the C/O ratio from given initial values until a reasonable fit to the observed spectrum is found. For the effective temperature, initial values were derived as the average temperature obtained from the calibrations of $(V - K)_0$, $(H - K)_0$ and $(J - K)_0$ vs. T_{eff} according to Bergeat et al. (2001). For a given object, the typical dispersion in the T_{eff} derived from the three indexes was ± 200 K for the late-R stars and ± 500 K for early-R stars. However, in the case of the early-R stars, the theoretical spectra are so sensitive to a small variation of the T_{eff} , that the uncertainty in the temperature is certainly much lower than $\sim \pm 500$ K. The spectroscopic method of deriving the effective temperature is not recommended in our case because of the blending with molecular lines, even in the warmer early-R stars. Further, the range in excitation energies of the apparently clean atomic lines available in our spectra is too narrow. Nevertheless, we checked that for the warmest early-R stars where the molecular contribution can be considered weak, we did not find any correlation between the estimated abundance of iron and the corresponding excitation energy of a number of Fe I lines (for instance in HIP 84 266, HIP 69 089 and HIP 39 118).

Gravity was estimated using the relation between luminosity, effective temperature and stellar mass. We adopted a mass of $1 M_{\odot}$ for all the stars in the sample. Although late-R stars are probably more massive (see Sect. 2.3), an uncertainty of a factor of two in the stellar mass translates to an uncertainty of

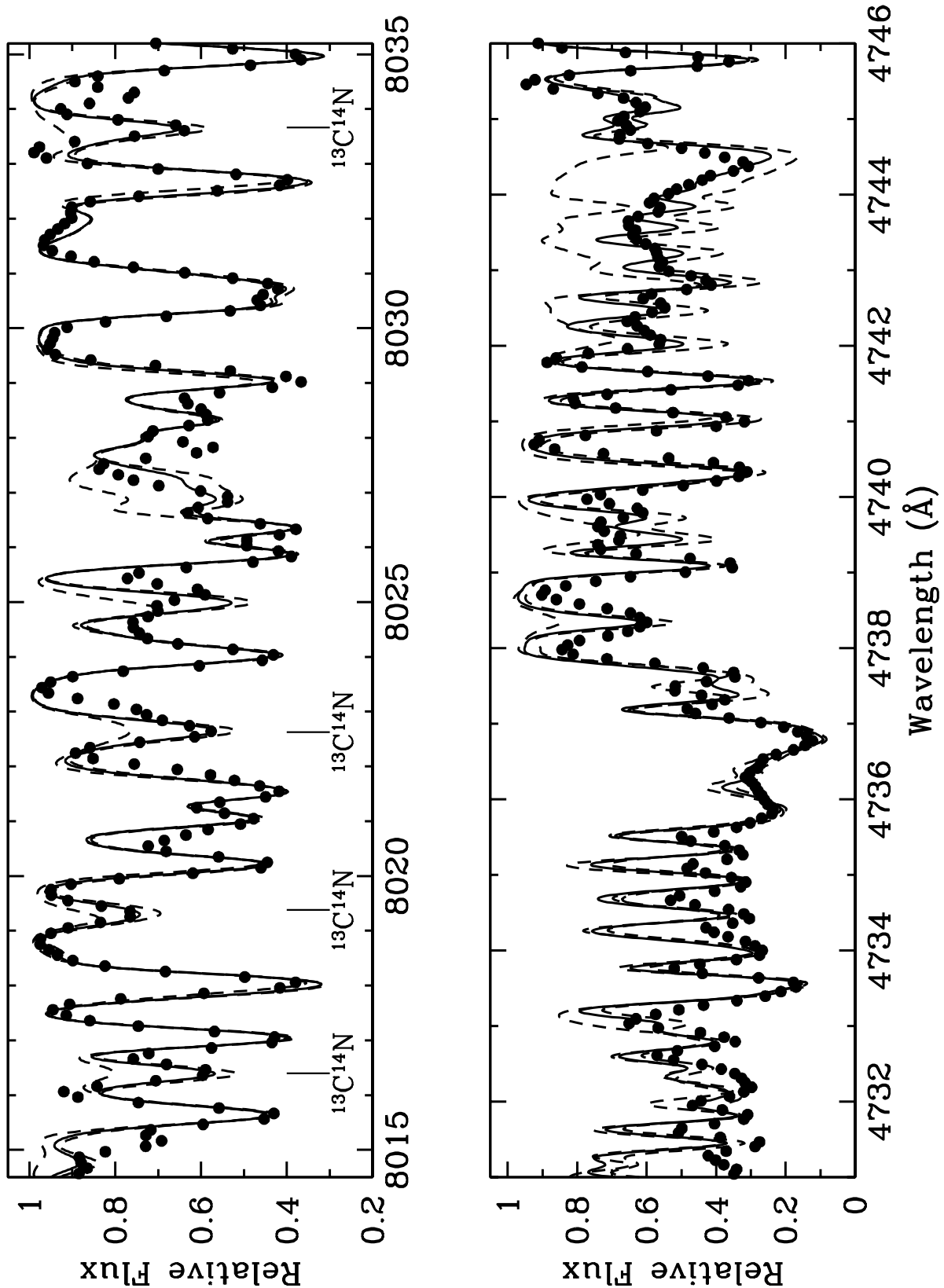


Fig. 3. Observed (filled circles) and synthetic spectra (continuous and dashed lines) of the early-R star HIP 84 266 around the λ 8015 Å (top), and the λ 4740 Å C_2 band regions (below), respectively. In both spectral ranges the synthetic spectrum giving the best fit (continuous line) was computed with $C/N/O = 8.78/8.40/8.56$ and $^{12}C/^{13}C = 7$. The position of some $^{13}C^{14}N$ lines used to derive the carbon isotopic ratio in the 8015 Å region are indicated. Dashed lines in both panels correspond to synthetic spectra computed with $^{12}C/^{13}C = 4$ and $^{12}C/^{13}C = 100$, respectively.

$\sim \pm 0.3$ dex in the gravity. Obviously, the most important source of uncertainty in the derived gravity is the luminosity. We estimate a maximum uncertainty in $\log g$ of $\sim \pm 0.9$ dex due to the combined uncertainty in the mass, effective temperature and luminosity. However, the theoretical spectra are very sensitive to such a variation in gravity, so the actual uncertainty in gravity is actually lower than this maximum value ($\sim \pm 0.5$). The mean difference between the estimated gravity and the final adopted value in the analysis was $\sim \pm 0.1$ dex for early-R stars. For late-R stars, the differences are below 0.5 dex except in the case of HIP 108 205 (0.9 dex).

We adopted initially a solar metallicity for all the stars according to the previous analysis by Dominy (1984). The reference solar abundances are those from Asplund et al. (2005). The final metallicity of the star ($[M/H]$) was obtained as the average derived from a number of Fe, Ni, Mn and Zn lines. For solar-metallicity and moderate metal-poor stars these species scale approximately with Fe (i.e. $[X/Fe] \sim 0.0$), thus, these elements can be safely used as metallicity indicators. The metallicity deduced from the $[X/H]$ ratios (with $X = \text{Fe, Ni, Mn and Zn}$) agreed within ± 0.05 for the early-R stars and ± 0.10 for the late-R stars. A microturbulence parameter of 2 km s^{-1} was adopted in all the stars, which is a typical value for giant stars. This initial value was modified in the chemical analysis by fitting the profile of metallic lines apparently free of molecular blends. We note that the microturbulence velocity giving the best fit to the observed spectrum may change slightly with the wavelength range. The average microturbulence velocities are given in Table 3. The macroturbulence velocity adopted was between $5 - 10 \text{ km s}^{-1}$. Finally, the theoretical spectra were convolved with a gaussian distribution to mimic the instrumental profile. The final FWHM values adopted were within $\sim 200 - 400 \text{ m}\text{\AA}$, depending on the wavelength range and the spectral resolution.

In the analysis of carbon stars a critical issue is the determination of the C, N, and O abundances since the actual C/O ratio in the atmosphere determines the dominant molecular bands and thus the global spectrum. The actual N abundance has a minor role in this sense. Unfortunately the O abundance is very difficult to measure in carbon stars at visual wavelengths. Only in two early-R stars in our sample, HIP 39 118 and HIP 62 944, it was possible to derive the O abundance from the $\lambda 6300.3 \text{ \AA}$ [OI] line. For the other stars, the O abundance was scaled with the average metallicity. We note that Dominy (1984) derived almost scaled to solar O abundances from molecular lines in the infrared in his sample of early-R stars. Nevertheless, the effect of the absolute O abundance on the theoretical spectrum is secondary with respect to the actual C/O ratio. This is because for a given C/O ratio (or difference $[C/H] - [O/H]$), there is a range of absolute O abundances (within a factor of three) giving almost equal theoretical spectra (see de Laverny et al. 2006). To estimate the C and N abundances, we proceeded as follow: first, the carbon abundance was derived from the C_2 Swan band lines at $\lambda\lambda 4730 - 4750 \text{ \AA}$ taking the nitrogen and oxygen abundances scaled with the average metallicity (except in the case of O for the two early-R stars mentioned above). The intensity of these C_2 lines are not very sensitive to the N and O abundances adopted. From this region we also derive the $^{12}\text{C}/^{13}\text{C}$ ratio from some available $^{12}\text{C}^{13}\text{C}$ and $^{13}\text{C}^{13}\text{C}$ lines. Next, we synthesize the region at $\lambda\lambda 8000 - 8050 \text{ \AA}$, which is dominated by the red system of CN molecule, to estimate the N abundance adopting the C abundance from the previous step. Then, we returned to the $\lambda\lambda 4730 - 4750 \text{ \AA}$ region to check the consistency of the theoretical and observed spectrum with the new N abundance derived.

Table 3. Atmospheric parameters and C, N, O abundances

Star	T_{eff} (K)	$\log g$	ξ (km s^{-1})	[M/H]	C	N	O
Late-R stars							
HIP 35 810	3300	0.0	2.8	-0.38	8.40	7.30 ^a	8.35
HIP 36 623	3300	0.0	2.1	-0.27	8.35	7.70	8.31
HIP 91 929	3300	0.0	2.5	0.00	8.68	7.78 ^a	8.66
HIP 108 205	2500	0.0	2.3	0.00	8.67	7.78 ^a	8.66
HIP 109 158	2500	0.0	2.5	-0.02	8.68	7.78 ^a	8.66
Early-R stars							
HIP 39 118	4250	2.0	1.8	-0.29	8.77	8.00	<9.05 ^b
HIP 44 812	3950	1.5	3.0	-0.03	8.75	8.70	8.66
HIP 53 832	4500	2.5	2.3	-0.77	8.08	8.10	8.06
HIP 58 786	4250	2.0	2.2	-0.29	8.63	7.60	8.47
HIP 62 944	4300	2.4	2.0	0.12	8.80	8.30	9.05 ^b
HIP 69 089	4750	1.5	2.0	-0.17	8.40	8.40	8.46
HIP 74 826	4750	2.0	1.5	-0.30	8.43	8.18	8.36
HIP 82 184	4500	2.0	3.0	-0.15	8.42	8.25	8.51
HIP 84 266	4750	2.0	2.4	-0.10	8.78	8.40	8.56
HIP 85 750	3800	1.2	2.0	-0.48	8.38	7.98	8.36
HIP 86 927	4700	2.4	2.3	-0.05	8.47	7.98	8.66
HIP 87 603	4100	2.0	2.3	-0.52	8.60	7.68	8.36
HIP 88 887	3950	1.5	3.0	-0.09	8.80	8.70	8.66
HIP 94 049	4100	2.0	2.3	-0.62	8.48	7.98	8.36
HIP 95 422	3950	2.0	3.0	-0.26	8.73	7.78 ^a	8.36
HIP 98 223	3800	1.5	1.9	-0.79	8.05	7.10	7.97
HIP 113 150	4500	2.0	2.4	-0.47	8.85	7.60 ^a	8.36

^a N abundance scaled with the stellar metallicity.

^b O abundance derived from the $\lambda 6300.3 \text{ \AA}$ [O I] line using the atomic line parameters from Caffau et al. (2008).

This procedure was repeated several times until convergence was found. Typically two or three iterations were needed. For a given star, the maximum difference between the C and N abundances derived from the red and blue parts of the spectrum was less than 0.2 or 0.1 dex for the early- and late-R stars, respectively. The final carbon isotopic ratio obtained is the average value between those obtained from the fits to the $\lambda \sim 8000 \text{ \AA}$ and $\lambda \sim 4750 \text{ \AA}$ regions. The final C, N and O abundances together with the other atmospheric parameters are shown in Table 3.

Synthetic spectra in LTE were computed for a specific star using the version 7.3 of the *Turbospectrum* code (Alvarez & Plez 1998). We used the same extensive set of atomic and molecular lines as in Papers II and III and refer to these works for details. The list of lines is available from the authors upon request. Figures 3 to 5 show examples of theoretical fits in four different spectral regions used in the chemical analysis. The lithium abundance was derived using the resonant Li I at $\lambda 6707.8 \text{ \AA}$. This spectral range is also interesting because of the presence of one useful Y I line at $\lambda 6687.5 \text{ \AA}$. For most of the stars in the sample, the Li abundance has to be considered only as an upper limit. This is due to the severe blending in this spectral region, as can be seen clearly in Fig. 4. *s*-element abundances were determined mainly using the spectral window at $\lambda\lambda 4750 - 4950 \text{ \AA}$ (see Papers II and III) where several lines of Sr, Y, Zr, Ba, La, Nd and Sm are present (see Fig. 5). For early-R stars we also used the Ba I-II lines at $\lambda 6498.9$ and $\lambda 6496.9 \text{ \AA}$, respectively. We attempted to detect the radioactive element technetium from the resonant lines at $\lambda 4260 \text{ \AA}$ and the recombination Tc I line at $\lambda 5924.5 \text{ \AA}$. We fail to detect the bluer line in all the stars mainly because of the low S/N ratio achieved in the spectra in that re-

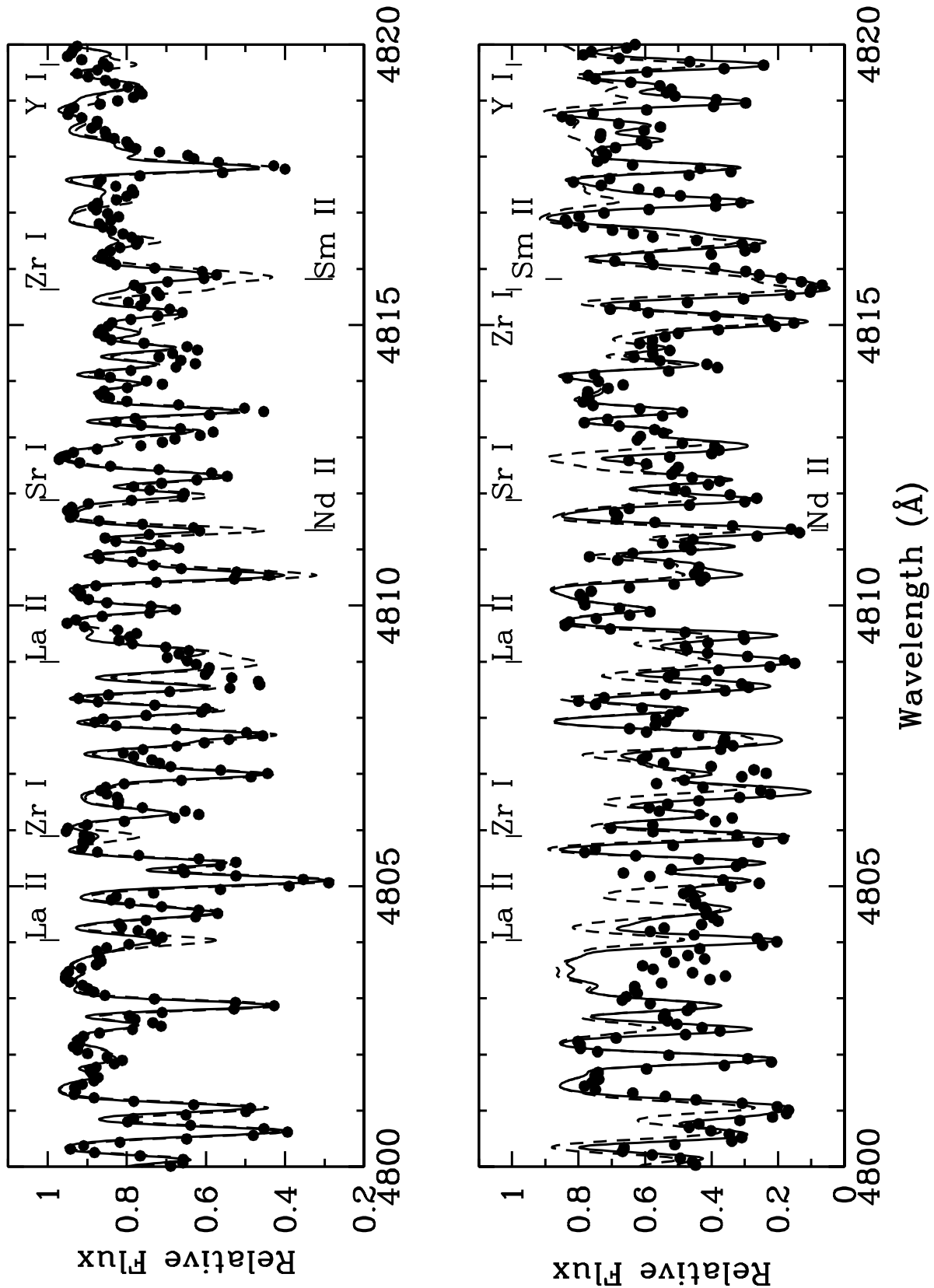
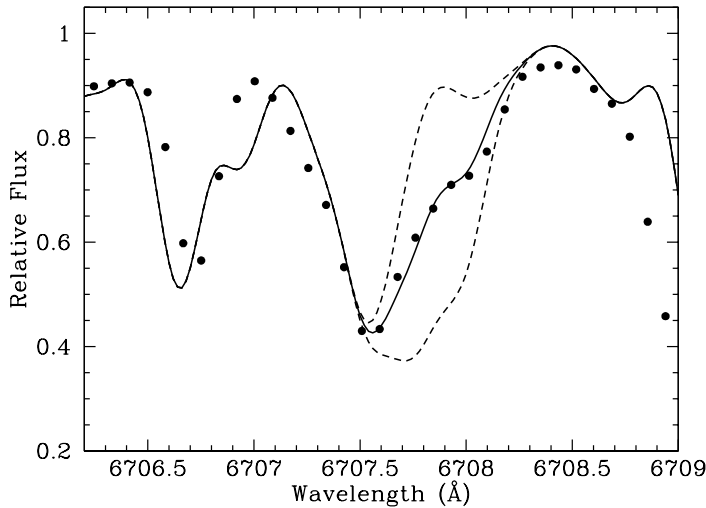


Fig. 5. Observed and synthetic spectra in the λ 4800 Å region for the early-R star HIP 84 266 (top panel) and the late-R star HIP 36 623 (bottom). Symbols as in Fig. 3. For each star two theoretical fits are shown: continuous line (best fit) is computed assuming $[s/M] \sim 0.0$, while dashed line with $[s/M] \sim +0.5$ in the star HIP 84 266. For HIP 36 623, continuous line is computed with $[s/M] \sim +1.3$ and dashed line with $[s/M] \sim 0.0$.

Table 4. Dependence of the derived abundances on the atmospheric parameters

Species X	T_{eff}^a $\pm 150/250\text{K}$	$\log g$ ± 0.5	$[M/H]$ ± 0.2	ξ $\pm 0.5 \text{ km s}^{-1}$	macro. $\pm 1.5 \text{ km s}^{-1}$	C/O ± 0.1	$^{12}\text{C}/^{13}\text{C}$ ± 10	Total
Late-R stars								
Li	± 0.40	± 0.05	± 0.20	∓ 0.00	± 0.00	∓ 0.20	± 0.00	± 0.50
Fe	± 0.30	± 0.00	-	∓ 0.05	± 0.10	∓ 0.10	± 0.00	± 0.35
Rb	± 0.20	± 0.10	± 0.20	∓ 0.00	± 0.00	∓ 0.15	∓ 0.10	± 0.35
Sr	± 0.15	± 0.00	± 0.10	∓ 0.05	± 0.20	∓ 0.10	∓ 0.05	± 0.30
Y	± 0.15	± 0.00	± 0.10	∓ 0.20	± 0.25	∓ 0.05	± 0.00	± 0.35
Zr	± 0.05	± 0.00	± 0.05	∓ 0.20	± 0.25	∓ 0.00	± 0.00	± 0.35
Ba	± 0.15	± 0.10	± 0.10	∓ 0.05	± 0.00	± 0.00	± 0.00	± 0.25
La	± 0.05	± 0.20	± 0.10	∓ 0.10	± 0.20	∓ 0.05	± 0.00	± 0.35
Nd	± 0.05	± 0.20	± 0.05	∓ 0.20	± 0.20	∓ 0.05	± 0.00	± 0.35
Sm	± 0.05	± 0.10	± 0.10	∓ 0.25	± 0.20	∓ 0.00	± 0.00	± 0.35
Early-R stars								
Li	± 0.10	± 0.00	± 0.10	∓ 0.00	± 0.00	∓ 0.10	± 0.05	± 0.30
Fe	± 0.05	± 0.00	-	∓ 0.05	± 0.15	∓ 0.10	± 0.00	± 0.20
Rb	± 0.05	± 0.00	± 0.00	∓ 0.00	± 0.05	∓ 0.05	± 0.00	± 0.20
Sr	± 0.10	± 0.00	∓ 0.05	∓ 0.10	± 0.15	∓ 0.05	∓ 0.00	± 0.20
Y	± 0.10	± 0.00	± 0.25	∓ 0.00	± 0.10	∓ 0.15	± 0.00	± 0.40
Zr	± 0.10	± 0.00	± 0.00	∓ 0.00	± 0.10	∓ 0.05	± 0.00	± 0.30
Ba	± 0.10	± 0.10	± 0.20	∓ 0.00	± 0.10	∓ 0.05	± 0.00	± 0.30
La	± 0.05	± 0.20	± 0.10	∓ 0.00	± 0.15	∓ 0.05	∓ 0.00	± 0.30
Nd	± 0.15	± 0.20	± 0.05	∓ 0.05	± 0.20	∓ 0.00	∓ 0.00	± 0.40
Sm	± 0.15	± 0.20	∓ 0.10	∓ 0.00	± 0.15	∓ 0.00	∓ 0.00	± 0.35

^a See text for details.**Fig. 4.** Observed and synthetic spectra in the region of the Li line at $\lambda \sim 6707.8 \text{ \AA}$ for the early-R star HIP 58 786. Symbols as in Fig. 3. Continuous line is the best fit with $\log \epsilon(\text{Li}) = 1.0$, and dashed lines are theoretical spectra computed with $\log \epsilon(\text{Li}) = 0.0$ and 1.5 , respectively.

gion. Upper limits on the Tc abundance were set in the stars HIP 39 118 and HIP 109 158 by using the recombination line. This result is compatible with the presence of some *s*-element enhancement (see Table 6) in these two stars. However, because we can barely reproduce the blend at $\lambda 5924 \text{ \AA}$, these Tc upper limits have to be taken with caution. Finally, Rb abundances were determined using the Rb I line at $\lambda 7800.2 \text{ \AA}$. In this region there are two Ni I lines at $\lambda 7788.9, 7797.6 \text{ \AA}$ and three Fe I

lines at $\lambda\lambda 7780.6, 7802.5, \text{ and } 7807.9 \text{ \AA}$ not very much blended by molecular absorptions that can be used to derive the average metallicity.

Table 4 shows the uncertainty in the abundances derived for the different chemical species due to the uncertainty in the model atmosphere parameters. To do this a canonical model atmosphere with parameters $T_{\text{eff}}/\log g/[M/H] = 4750/2.0/0.0$ and $3300/0.0/0.0$ was used for early- and late-R stars, respectively. Due to the very different sensitivity of the theoretical spectra to changes in the effective temperature, changes in the abundances due to this parameter were calculated assuming variations by ± 150 and $\pm 250 \text{ K}$ for early- and late-R stars, respectively.

The final uncertainty in the abundance is found by considering quadratically all the uncertainties including the uncertainty in the continuum position ($< 5\%$) and, when more than 3 lines of a given element were used, the abundance dispersion among the lines of this element as an additional source of uncertainty. This is indicated in the last column of Table 4. From this table it can be appreciated that the error in the absolute abundances derived are in the range $\Delta[X/H] = \pm(0.2 - 0.5)$ dex, being larger for late-R stars. When considering the abundances ratios ($[X/\text{Fe}]$) relative to iron, the error is reduced if the variation on a given atmospheric parameter affects in the same way the element of interest. The results of the chemical analysis are summarised in Tables 5 and 6. The last four columns in Table 6 show the average enhancement of light *s*-elements, $ls = \langle \text{Sr}, \text{Y}, \text{Zr} \rangle$, heavy *s*-elements, $hs = \langle \text{Ba}, \text{La}, \text{Nd}, \text{Sm} \rangle$, the *s*-element index $[hs/ls]$, and the total average *s*-element enhancement.

Table 5. Abundances derived and relevant abundances ratios.

Name	C/O	$^{12}\text{C}/^{13}\text{C}$	Li	Mn	Fe	Ni	Zn	[M/H]	[C/M]	[N/M]
Late-R stars										
HIP 35 810	1.12	65	0.20	-	7.07	5.93	4.20	-0.38	0.39	-
HIP 36 623	1.10	23	-0.20	-	7.18	5.92	-	-0.27	0.23	0.19
HIP 62 401	-	-	-	-	-	-	-	-	-	-
HIP 91 929	1.05	58	-0.50	-	7.45	6.23	-	0.00	0.29	-
HIP 108 205	1.02	90	-1.50	-	7.45	-	-	0.00	0.28	-
HIP 109 158	1.05	85	-1.00	-	7.43	5.93	-	-0.02	0.31	-
Early-R stars										
HIP 39 118	>0.50	13:	0.85	5.10	7.16	5.93	-	-0.29	0.67	0.51
HIP 44 812	1.23	5	<1.00	-	7.42	6.23	4.60	-0.03	0.39	0.95
HIP 53 832	1.05	24	<0.60	4.69	6.68	5.43	3.80	-0.77	0.46	1.09
HIP 58 786	1.45	70	<1.00	-	7.16	5.90	4.15	-0.29	0.53	0.11
HIP 62 944	0.56	22	2.60	5.49	7.57	6.28	4.70	0.12	0.29	0.40
HIP 69 089	0.87	19	1.80	5.25	7.28	6.04	4.50	-0.17	0.18	0.79
HIP 74 826	1.17	20	<0.50	5.10	7.15	5.95	4.30	-0.30	0.34	0.70
HIP 82 184	0.81	10	<0.40	5.24	7.30	6.08	4.45	-0.15	0.18	0.62
HIP 84 266	1.65	7	<1.05	5.29	7.35	6.13	4.50	-0.10	0.49	0.72
HIP 85 750	1.05	22	<0.30	4.89	6.97	6.97	<3.85	-0.48	0.47	0.68
HIP 86 927	0.65	7	<0.48	5.35	7.40	7.40	<4.55	-0.05	0.13	0.25
HIP 87 603	1.74	9	<1.10	-	6.93	6.93	4.20	-0.52	0.73	0.42
HIP 88 887	1.38	5	<0.50	-	7.36	7.36	4.30	-0.09	0.50	1.01
HIP 94 049	1.32	9	<0.40	-	6.83	6.83	-	-0.62	0.71	0.82
HIP 95 422	2.34	6	<0.50	-	7.19	7.19	-	-0.26	0.60	-
HIP 98 223	1.20	16	<0.00	-	6.66	6.66	-	-0.79	0.45	0.11
HIP 113 150	3.09	9	<0.55	-	6.98	6.98	-	-0.47	0.93	-

: indicates uncertain value.

4. Results and discussion

4.1. Comments on particular stars

The detailed chemical composition reported in Tables 5 and 6 shows that there are several stars that do not fulfil one of the main characteristic that defines a R star, i.e., a carbon star without *s*-element enhancements. HIP 39 118 is one of these stars, showing a clear *s*-element enhancement, $[s/M] \sim +0.54$. In fact, our best fit to the Tc I line at λ 5924 Å in this star gives $\log \epsilon(\text{Tc}) < 1.20$. This, together with the *s*-element enhancement found would be an indication of this star being on the AGB phase. However considering that the luminosity of this star is too low to be on the AGB phase (see Table 2), and the difficulty in reproducing the λ 5924 Å Tc blend, this Tc upper limit has to be considered with extreme caution and thus, it would be risky to conclude that HIP 39 118 is an AGB star. HIP 39 118 has other chemical peculiarities. It is not a carbon star since its C/O ratio (~ 0.50) is considerably lower than unity even considering the uncertainty in the derivation of this ratio. Indeed, the λ 6300 Å [OI] line is very strong in this star which indicates some O enhancement, $[O/Fe] < 0.68$. Titanium, another alpha element, is also enhanced in this star $[\text{Ti}/\text{Fe}] = +0.3$. Due to its low luminosity ($M_{\text{bol}} = 0.47$) and *s*-element enhancement one is tempted to ascribe this star as a classical barium star that are known to be all binaries. In the case of HIP 39 118, there are only two radial velocity measurements within a 5 days interval separation (Platais et al. 2003). With such short time span compared with the long orbital periods of the classical barium stars, no conclusion may be drawn regarding binarity. Moreover, the moderate Li abundance in this star, $\log \epsilon(\text{Li}) = 0.85$, is difficult to explain

in a mass transfer scenario. Thus, the spectral classification of this star is uncertain and we just put it in the group of chemically anomalous red giant stars, but certainly not an early-R star.

HIP 53 832 has an abundance pattern typical of a classic CH-type star: a moderate metal-poor carbon-rich ($[M/H] = -0.77$, $C/O = 1.05$) star with a relatively low carbon isotopic ratio, ($^{12}\text{C}/^{13}\text{C} = 24$) and an important *s*-element enhancement ($[s/M] = +1.26$). In fact, the binary nature of this star has been confirmed by radial velocity measurements by Platais et al. (2003) and thus, there is no doubt about its classification as a CH star.

HIP 62 944 is one of the first Li-rich giants discovered (Wallerstein & Sneden 1982). Our Li abundance in this star, $\log \epsilon(\text{Li}) = 2.60$, agrees with that deduced by these authors. The CNO content and the metallicity derived here are also in agreement. Again this star is not a carbon star as the C/O ratio is near the solar value (see Table 5). The low isotopic ratio ($^{12}\text{C}/^{13}\text{C} = 22$) derived here is similar to those found in others Li-rich giants (de La Reza 2006). The origin of Li in RGB stars is not well understood. Some kind of non-standard mixing mechanism during the RGB phase (see e.g. Palacios et al. 2001, 2006; Guandalini et al. 2009) seems to be needed. In any case, HIP 62 944 is a K giant, not a R star.

HIP 69 089 presents some C enrichment although its C/O ratio is below unity (0.87, see Table 5). As in the case of HIP 62 944, this star is also Li-rich ($\log \epsilon(\text{Li}) = 1.80$) with a low carbon isotopic ratio (19) typical in these stars. The Li abundance previously derived by Luck & Challener (1995) in this star, $\log \epsilon(\text{Li}) = 2.04$, is compatible with the value derived in the present work. The *s*-element abundances are solar scaled. On the basis of these values we classify it as another Li-rich K giant.

Table 6. Heavy element abundance ratios.

Name	[Rb/M]	[Sr/M]	[Y/M]	[Zr/M]	[Ba/M]	[La/M]	[Nd/M]	[Sm/M]	[ls/M]	[hs/M]	[hs/ls]	[s/M]
Late-R stars												
HIP 35 810	-	0.26	0.27	0.29	0.78	0.55	0.83	0.17	0.27	0.58	0.31	0.43
HIP 36 623	0.10	0.95	1.31	1.13	1.72	1.64	1.72	0.56	1.13	1.41	0.28	1.27
HIP 91 929	-	-	-0.01	0.01	-0.02	-	-	-	0.00	-0.02	-0.02	-0.01
HIP 108 205	-	-	0.59	-	0.73	-	-	-	0.59	0.73	0.14	0.66
HIP 109 158	-	-	0.81	-	0.85	-	-	-	0.81	0.85	0.04	0.83
Early-R stars												
HIP 39 118	0.30	0.22	0.68	0.70	0.49	0.46	0.64	0.58	0.53	0.54	0.01	0.54
HIP 44 812	-	-0.07	0.03	-0.26	-0.04	0.13	-	0.12	-0.10	0.07	0.17	-0.01
HIP 53 832	<0.70	0.85	1.06	0.78	1.65	<2.04	1.42	1.36	0.90	1.62	0.72	1.26
HIP 58 786	-	0.09	-0.06	-0.30	0.02	-0.01	-	-0.01	-0.09	0.00	0.09	-0.04
HIP 62 944	-0.09	-0.02	-0.17	-0.41	-0.29	-0.02	-0.12	0.07	-0.20	0.09	0.11	-0.15
HIP 69 089	-0.13	0.05	0.16	-0.12	0.00	0.07	0.07	0.06	0.03	0.05	0.02	0.04
HIP 74 826	0.01	-0.02	0.02	0.01	0.08	-0.04	0.00	-0.01	0.00	0.01	0.00	0.01
HIP 82 184	-0.01	0.00	-0.07	-0.14	0.08	0.15	-0.10	0.00	-0.07	0.03	0.10	-0.02
HIP 84 266	-0.04	0.00	-0.21	-0.11	-0.07	0.22	0.05	0.14	-0.11	0.09	0.19	-0.01
HIP 85 750	-0.05	0.76	0.97	0.59	1.56	1.65:	1.53	1.27	0.77	1.45	0.68	1.11
HIP 86 927	0.18	0.00	-0.01	0.31	0.20	0.32	0.40	0.19	0.10	0.28	0.18	0.19
HIP 87 603	0.05	0.12	0.11	-0.07	0.45	0.52	0.12	0.11	0.05	0.30	0.25	0.18
HIP 88 887	-0.07	-0.13	-0.02	-0.20	-0.18	-0.11	-0.11	-0.12	-0.12	-0.13	-0.01	-0.12
HIP 94 049	-	-	0.02	-	-0.05	-	-	-	0.02	-0.05	-0.07	-0.01
HIP 95 422	-	-	-0.04	-	0.11	-	-	-	-0.04	0.11	0.15	0.04
HIP 98 223	-	0.67	1.13	1.00	1.25	-	1.44	1.18	0.93	1.29	0.36	1.11
HIP 113 150	-	-	-0.03	-0.02	0.00	-	-	-0.04	-0.02	-0.02	0.00	-0.02

ls = (Sr, Y, Zr), hs = (Ba, La, Nd, Sm) and s = (ls + hs).

We derive significant *s*-element overabundances in the carbon star HIP 85 750 (see Table 6). Radial velocity variations have been detected in this star (Table 1). Since it is a moderately metal-poor star, we classify it as a CH-type star.

According to our analysis HIP 86 927 is not a carbon star ($C/O = 0.65$), and shows no *s*-element enhancement. Its carbon isotopic ratio is low (7) and agrees with the previous determination by Dominy (1984). Unfortunately, this author did not derive any other abundance signature in this star. Further, the luminosity of this star ($M_{bol} = 0.22$) is too low for a typical early-R star (see Sect. 2.6), thus we believe that its characteristics are closer to a normal K giant which has undergone some extra-mixing revealed by its low $^{12}C/^{13}C$ ratio.

Finally, HIP 98 223 is a metal-poor ($[M/H] = -0.79$) carbon star showing a large enrichment in *s*-elements ($[s/M] = +1.11$). These are the typical abundance signatures of the CH stars.

Among the late-R stars we have two *peculiar* stars. HIP 36 623 is a symbiotic star (Johnson et al. 1988; Belczyński et al. 2000; Munari & Zwitter 2002) whose luminosity (see Table 2) and chemical composition (see Tables 5 and 6) are compatible with those expected at the AGB phase. Perhaps the envelope of this star has undergone two periods of mixing: the first one by the material accreted from the primary star, and the second one, a self-contamination triggered by third dredge-up episodes on the AGB phase. Thus, it is probably a normal N-type star. The spectrum of this star looks similar to the other late-R in the sample without any evidence of contamination by emission lines or emission continua coming from the hot UV radiation of the companion (probably a white dwarf). The broad emission features around 6825 and 7082 Å (due to O VI photons Raman scattered

off H I) are not present either. These features are found in some symbiotic stars (e.g. AG Dra, Smith et al. 1996). Thus, we believe that the abundances of the *s*-elements in this star (mostly derived from the blue part of the spectrum) are not underestimated because of a contribution to the spectral continuum by the companion star. On the other hand, we do not find *s*-element overabundances in the late-R HIP 91 929. However its spectrum is identical to those of N-type stars. In Paper II we found a few N-type stars where the *s*-element content was compatible with no enhancements within the error bars. Perhaps HIP 91 929 is another example of this. Maybe these stars are at the beginning of the thermally pulsing AGB phase (as their luminosity might indicate) and did not have time yet to pollute the envelope with *s*-elements.

In summary, out of seventeen stars classified as early-R stars we have found seven stars ($\sim 40\%$) that are not R stars. Since the stars in our sample were randomly chosen from the Hipparcos catalogue (the only condition was to be observable from the north hemisphere) and although the sample is limited, we confirm the previous claims that among the R stars there is a significant number of stars which are wrongly classified. This is an important result since it might discard the previous belief (see Sect. 1) that the R stars (namely early-R) represent a frequent stage in the evolution of low-mass stars.

4.2. C/O and $^{12}C/^{13}C$ ratios

Fig. 6 shows the C/O and $^{12}C/^{13}C$ ratios found in our stars ($C = ^{12}C + ^{13}C$). The stars reclassified here (see previous section) are indicated by open symbols (squares, CH stars and trian-

gles, K giants) In the figure are indicated the expected values of the $^{12}\text{C}/^{13}\text{C}$ ratio according to standard low-mass stellar models (e.g. Cristallo et al. 2009) after the first dredge-up, and the AGB phase, respectively. The expected range in the AGB phase has been computed considering the effect of an extra-mixing mechanism after the first dredge-up (Boothroyd & Sackmann 1999), which would reduce further the $^{12}\text{C}/^{13}\text{C}$ ratio to a typical value of ~ 12 . Such $^{12}\text{C}/^{13}\text{C}$ ratios are frequently found in Population I giant stars (Gilroy 1989; Gilroy & Brown 1991) and can be only explained assuming a non standard mixing process (Charbonnel et al. 1998). It is evident from Fig. 6 that most of the *true* early-R stars have carbon isotopic ratios far below the minimum values expected after the first dredge-up (RGB phase) and the thermally pulsing AGB phase. Further, since early-R stars show also N enhancements (see Table 5, and Dominy 1984), the low $^{12}\text{C}/^{13}\text{C}$ ratios together with the N overabundances ($\langle [N/M] \rangle = +0.6$) would indicate that the material in the envelope of these stars has been processed through the CNO bi-cycle (almost at the equilibrium). If that were the case, material exposed to the CNO bi-cycle is expected to be depleted in ^{16}O by a factor of at least ~ 40 , the exact value depending on the burning temperature. Even considering the large uncertainty in the O abundance in our stars (actually we scale the O abundance with the average metallicity, see Sect. 3), we can safely discard a large O depletion from the analysis: the C/O ratios would be much higher than the values found here and because few C would be locked into CO, the C-bearing molecules (CN, CH and C_2) would appear very strong in the spectrum which is not observed in any of the early-R stars. Furthermore, for the few early-R stars where O abundance has been determined (Dominy 1984) no evidence of oxygen depletion is found. This fact casts some doubt on the idea that the mixing of CNO-equilibrium material is the only responsible for the early-R stars. The C and N enhancements found are rather evidence that the material that we currently observe in the envelopes of early-R stars has been processed by both the CN cycle and He-burning. Probably, C-rich material was mixed with protons on a time scale short enough and at a temperature low enough ($T \leq 7 \times 10^7$ K) to allow only the reactions $^{12}\text{C}(p, \gamma)^{13}\text{C}$ and $^{13}\text{C}(p, \gamma)^{14}\text{N}$, without any significant operation of the ON-cycle. In any case, the determination of the oxygen isotopic ratios in early-R stars would be a valuable tool to evaluate the role played by the CNO bi-cycle in the surface composition of these stars.

On the other hand, the $^{12}\text{C}/^{13}\text{C}$ ratios derived in late-R stars are significantly higher than those for the early ones. In these stars observations in general agree with AGB model predictions (see Fig. 6). An exception is the star HIP 36 623 with a $^{12}\text{C}/^{13}\text{C}$ ratio below the predicted values for the AGB carbon stars. However, these low $^{12}\text{C}/^{13}\text{C}$ values have been found also in many N-type stars (Ohnaka & Tsuji 1996; Abia et al. 2002) and are currently interpreted as an evidence of the operation of a non standard mixing process also in low-mass stars during the AGB phase. Differences between the early- and late- R stars are also evident in the C/O ratio. Early-R stars show a wider range in the C/O ratio while late-R stars are concentrated very close to 1, as in the galactic N-type stars of similar metallicity (Lambert et al. 1986; Abia et al. 2002). This is consistent with late-R stars having higher mass than early-R stars because it is more difficult to increase the C/O ratio of a more massive star.

4.3. Lithium

As noted in Sect. 3, most of the Li abundances derived in early-R stars should be considered upper limits. In cooler late-R stars,

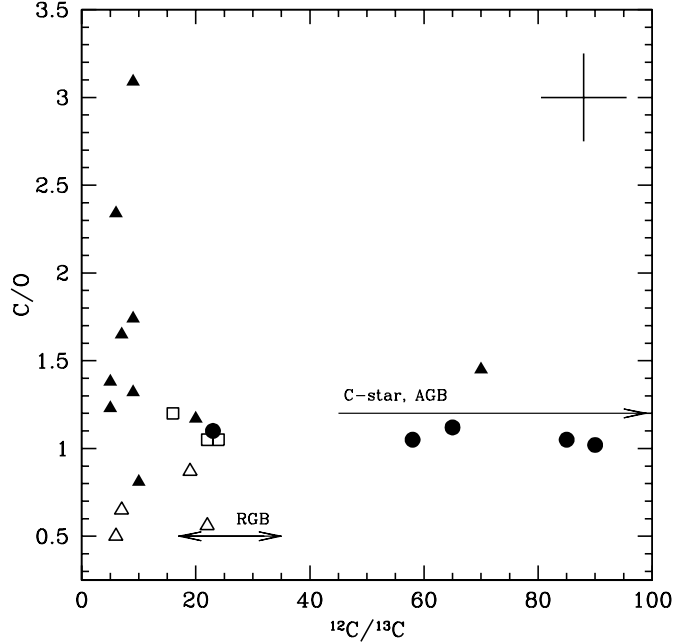


Fig. 6. C/O vs. $^{12}\text{C}/^{13}\text{C}$ ratios. Symbols as Fig.2. The arrows indicate the expected range in the $^{12}\text{C}/^{13}\text{C}$ ratio according to the standard evolutionary models of low-mass stars in the RGB and AGB phases (see text for details).

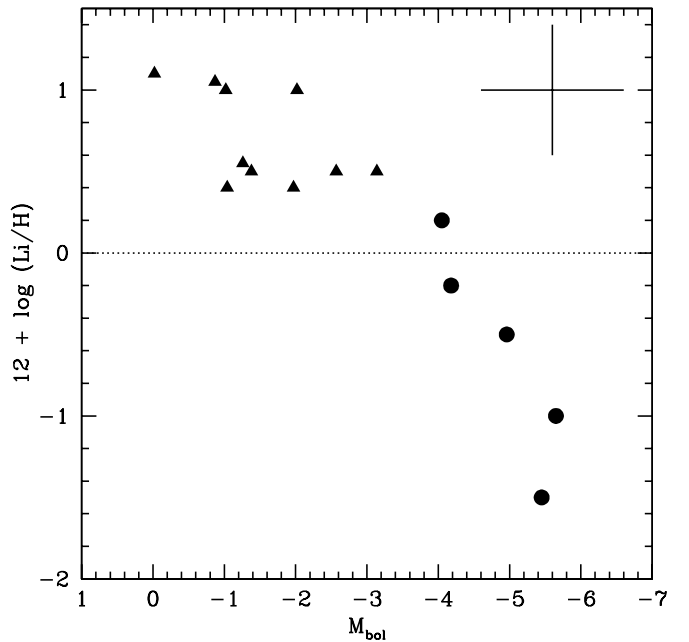


Fig. 7. Derived Li abundances and the absolute bolometric magnitude according to Bergeat et al. (2002a). Symbols as in Fig. 2.

synthetic spectra are much more sensitive to changes in the Li abundance (but note however the large formal uncertainty in the Li abundance, see Table 4). Fig. 7 presents the Li abundances derived in late- and early-R stars (excluding the stars reclassified in the previous section) and the luminosity. We remind that the typical stellar mass of early- and late-R stars is probably very

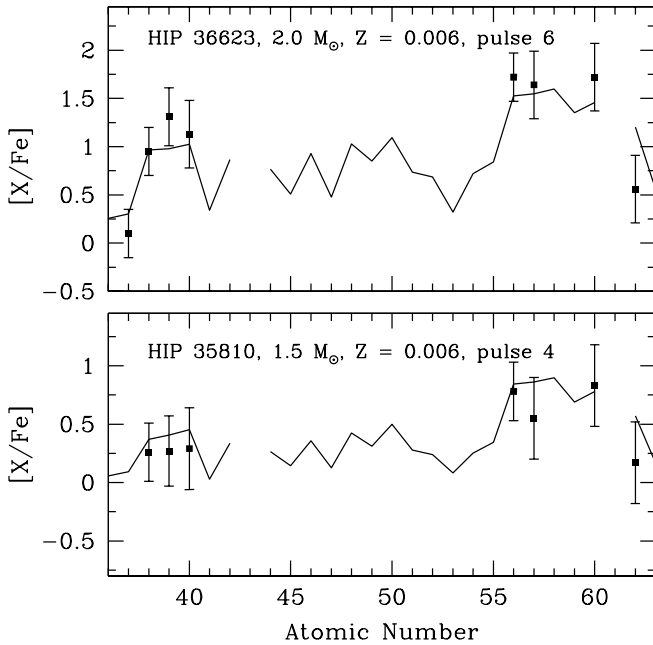


Fig. 8. Comparisons of the derived s -element ratios ($[X/Fe]$) in the late-R stars HIP 36 623 and HIP 35 810 with the theoretical predictions by Cristallo et al. (2009) for two different low-mass AGB models. In each panel is indicated the stellar mass, metallicity and specific thermal pulse that provide the best fit to the observed abundances.

different (see Sect. 2.3) thus, one should not establish a sequence of Li depletion in R stars from this figure. Instead, the apparent Li abundance vs. luminosity relationship have to be interpreted separately. By comparing stars of the same spectral type we found that early-R stars present very similar Li abundances (in the range $\log \epsilon(\text{Li}) \sim 0.5 - 1.0$) without any evident correlation with the luminosity. These upper limits in the Li abundances are higher than the expected values in post-tip RGB stars (marked with the dotted line at $\log \epsilon(\text{Li}) = 0.0$ in Fig. 7, e.g. Castilho 2000). Although, it would be necessary to confirm the possible Li detection with higher resolution spectra, this is of some relevance because it may constrain the scenarios proposed to form a R star.

In late-R stars, at contrary, Li abundances decrease with the increasing luminosity as one would expect to occur as the stellar envelope goes deeply toward the interior of the star during the ascend along the AGB phase. Indeed, the Li abundances derived in our late-R stars are similar to those derived in normal AGB carbon stars (Denn et al. 1991; Abia et al. 1993), which supports again the idea that they are identical to the N-type stars.

4.4. Abundances of heavy elements

Table 6 summarises the heavy element abundances derived in our stars. In the sample of early-R stars, and excluding those stars that we have reclassified as belonging to other spectral types (see above), it is evident that these stars do not have s -element overabundances $[X/M] \sim 0.0$ within the error bars. This is the case of HIP 44 812, HIP 58 786, HIP 74 826, HIP 82 184, HIP 84 266, HIP 87 603, HIP 88 887, HIP 94 049, HIP 95 422 and HIP 113 150. Thus, we confirm the analysis by Dominy

(1984) in this kind of stars. Late-R stars do have s -element enhancements⁴ at the same level than those found in galactic N-type stars of similar metallicity, $\langle [s/M] \rangle = 0.64$ (Abia et al. 2002). In fact, we detect Tc (using the weak recombination line at $\lambda 5924.47 \text{ \AA}$) in HIP 109 158 and it may be also present in HIP 108 205. This is usually interpreted as evidence of the *in situ* production of the s -elements in the star, the envelope being polluted by the operation of the third dredge-up during the AGB phase. These stars are named *intrinsic*. Fig. 8 shows an example of a detailed reproduction of the observed heavy element pattern in two late-R stars by theoretical s -process nucleosynthesis calculations in low-mass AGB stars. (see details in Cristallo et al. 2009). Each panel indicates the stellar mass model and thermal pulse giving the best fit to the observed pattern. The metallicity in the model (Z) was chosen as close as possible to the observed metallicity in the stars. By selecting a stellar mass model, metallicity and specific thermal pulse, fits of similar quality can be found for the other late-R stars in our sample, as well as for the early-R stars reclassified as CH-type (HIP 98 223, HIP 85 750 and HIP 53 832) which also show heavy element enhancements. In this case, we can mimic their extrinsic nature (i.e. the chemical composition of the envelope is due to the pollution by the matter accreted from a companion) including an extra-parameter in the model: the dilution factor, defined as the ratio between the mass of the envelope and the mass transferred from the primary star (e.g. Bisterzo et al. 2006). The dilution factor needed are in the range 2 – 3. These values are consistent with a secondary star having a large envelope, most of the CH-type star are indeed giants.

We close this section realising once more that the most probable neutron source producing the observed s -element pattern in these stars is the $^{13}\text{C}(\alpha, n)^{16}\text{O}$ reaction which is found the main neutron donor in low-mass AGB stars (Lambert et al. 1995; Abia et al. 2001). This is concluded from the observed $[\text{Rb}/\text{Sr}, \text{Y}, \text{Zr}] \leq 0$ (see Table 6). In AGB stars of intermediate mass ($M \geq 3 M_{\odot}$) probably dominates the $^{22}\text{Ne}(\alpha, n)^{25}\text{Mg}$ neutron source resulting in higher neutron densities ($N_n \geq 10^{10} \text{ cm}^{-3}$) and so $[\text{Rb}/\text{Sr}, \text{Y}, \text{Zr}] > 0$ (e.g. García-Hernández et al. 2006).

4.5. Evolutionary status

We have shown in the previous analysis that the true early- and late-R stars have different properties. Most of the late-R stars are long-period variables of the SR or Mira types (see Table 1), and they often exhibit excess emission at $12 \mu\text{m}$ due to dust, indicative of mass loss. In the colour-colour diagram they occupy the same location as N-type stars and have similar luminosities (or slightly lower). We have also shown that there is no significant difference in the chemical composition of late-R stars and N-type stars, both types showing s -element enhancements at the same level. They are thus closely related, or are identical. Definitely late-R stars are AGB stars and, most probably, mark the bottom of the AGB phase.

Concerning early-R stars, our study (although limited in the number of stars) confirms previous claims that most carbon stars catalogues contain a significant number of stars wrongly classified as early-R stars. In a sample of seventeen early-R stars we have found seven ($\sim 40\%$) objects that are K giants or CH-type stars. This finding, together with the definite ascription of late-R stars as N stars certainly reduce the number of real (early) R

⁴ The late-R star HIP 62 401 is excluded from the chemical analysis because its spectrum shows very broad lines that we cannot reproduce. This is typically found in Mira variables, see Table 1.

type stars among all the giant carbon stars. Therefore, R stars are indeed scarce objects, but we still lack an evolutionary scenario to explain their observational properties. We have to consider at least three possibilities: i) mass transfer in a binary system, ii) original pollution, and iii) a non-standard mixing mechanism able to mix carbon to the surface. Due to their position in the H-R diagram, and their peculiar chemical composition, the favoured scenario is the later one (Dominy 1984; Knapp et al. 2001) triggered by an anomalous He-flash (e.g. Mengel & Gross 1976; Paczynski & Tremaine 1977).

As noted in Sect. 1, all early-R stars seem to be single stars: so far, attempts to detect radial velocity variations due to binarity have failed (McClure 1997). This is indeed a very improbable figure since in any stellar population one would expect a minimum of $\sim 30\%$ binary systems. McClure (1997) used this argument to suggest that R stars were initially all binaries and that they coalesced into a single object during their evolution. In this hypothesis one might argue that the carbon enrichment that we currently observe was a consequence of mass transfer prior to the coalescence. However, it is extremely difficult to form carbon stars from mass transfer at near solar metallicity (Abia et al. 2003; Masseron et al. 2009, although a few exceptions seem to exist, e.g., BD +57° 2161, see Zacs et al. 2005), thus there is very little or not space for the mass transfer scenario. The second scenario (carbon excess in the original gas cloud) it also ruled out because one should expect to find carbon stars of near solar metallicity at earlier evolutionary stages (main sequence, turn-off, sub-giants stars etc.). This is the case of the carbon rich metal-poor stars discovered in the galactic halo (e.g. Aoki et al. 2007; Masseron et al. 2009): they are found along all the H-R diagram from the main sequence to the RGB. However, no a sole star with similar characteristics to those of early-R has been found in earlier evolutionary stages. In the same line, we might ask where are the descendants or early-R stars? Once leaving the He-core burning phase, they will evolve and ascend the giant branch for a second time, i.e. they should become AGB stars. The carbon stars of J-type have been traditionally proposed as the *daughters* of early-R stars (e.g. Lloyd Evans 1986) because of their chemical similarities (both are carbon stars without s-element enhancements) and the higher luminosity of the J-stars (typical of the AGB phase). The large Li abundances typically found in J-type stars ($\sim 80\%$ show $\log \epsilon(\text{Li}) > 0.5 - 1.0$, Paper I) are consistent with the Li excess that we have found here in early-R stars, supporting this idea. Nevertheless, this picture is far from clear since, for instance, the galactic distribution of the J-type stars is different from that of the early-R stars: J-type stars are located mainly in the galactic thin disk (only $\sim 17\%$ of the J-type stars studied by Chen et al. 2007 have galactic latitude values $|b| \geq 25^\circ$, typical of the thick disk stars). Secondly, a few J-type stars have been found in binary systems (e.g. BM Gem, EU And, UV Aur and UKS-Cel, Barnbaum et al. 1991; Belczyński et al. 2000). Further work is necessary to determine if early-R stars are, in fact, the progenitors of some of the J-type stars.

The solution seems to be related with the third scenario during or after the He-flash. However, as commented in Sect. 1, one-dimensional (1D) attempts and very recent three-dimensional (3D) numerical simulations of the He-flash for stars with a metallicity close to solar, as observed in early-R stars (Dearborn et al. 2006; Lattanzio et al. 2006; Mocák et al. 2008a,b), have fail to mix carbon with the envelope. Binary mergers have been suggested as the mechanism able to provoke an anomalous He-flash. In the merger, a fast rotating He core is supposed to be formed with, as a consequence, a strong off-

center He-flash. This stronger He-flash eventually would mix carbon to the surface. Izzard et al. (2007) explored statistically the different binary scenarios that might produce a R star. They discussed actually eleven possible channels, the most favourable cases being the merger of a He white dwarf with a RGB star and that of a RGB star with a Hertzsprung gap star. In fact, their binary population study produces ten times as many stars as required to match the early-R to red clump ratio observed. This discrepancy (that becomes more severe considering our results) was, however, interpreted by these authors as a positive result since they expect that only a very small fraction of the favourable systems would ignite He while rotating rapidly enough to provoke the conditions for carbon mixing into their envelope. We have tested this scenario by parametrised 1D simulations of the merging and, for the first dynamical part, by 3D Smoothed Particle Hydrodynamics (SPH) simulations. An extended discussion of these numerical simulations will be presented in an accompanying paper (Piersanti et al. 2009), but we can advance here that in the most favourable merging channels according to Izzard et al. (2007), we do not obtain any carbon mixing (see also Zamora 2009).

Very recently, Wallerstein et al. (2009) have found several carbon-rich ($\text{C/O} > 1$) RR Lyrae stars with similar N enhancements to those in early-R stars and have suggested that carbon might have mixed to the surface during the He-flash by an still unknown physical conditions. More theoretical work on this subject is needed to determine such conditions.

5. Summary

We have shown that the early- and late-type R stars have different properties including their chemical composition. Late-R stars have almost identical chemical figures than normal (N-type) AGB carbon stars, they occupy a similar position in the HR diagram, are long period variables and present infrared excesses due to dust. These stars probably mark the bottom of the AGB phase and can be considered thus identical to the N stars. For the early-type R stars we confirm the chemical features found in the early analysis by Dominy (1984) and the fact that many CH-type and/or K giants have been erroneously classified as early-type R stars in the available carbon stars catalogues. So early-type R stars are indeed rare objects accounting a much smaller fraction among the giant carbon stars than previously thought. The location of these stars in the red clump provides strong support for their formation through an anomalous He-flash that would mix carbon to the surface. However, all the theoretical attempts made up to date have fail to reproduce such mixing. The origin of early-type R stars still remains a mystery.

Acknowledgements. Part of this work was supported by the Spanish Ministerio de Ciencia e Innovación projects AYA2002-04094-C03-03 and AYA2008-04211-C02-02. OZ acknowledges support by the FPI grant and the Plan propio of University of Granada. We thank the referee, Dr. Jorissen, whose detailed comments have helped us to improve the paper. Based on observations collected at the Centro Astronómico Hispano Alemán (CAHA) at Calar Alto, operated jointly by the Max-Planck Institut für Astronomie and the Instituto de Astrofísica de Andalucía (CSIC). This work has made use of the SIMBAD database operated at CDS, Strasbourg, France.

References

- Abia, C., Boffin, H. M. J., Isern, J., & Rebolo, R. 1993, *A&A*, 272, 455
- Abia, C., Busso, M., Gallino, R., et al. 2001, *ApJ*, 559, 1117
- Abia, C., Domínguez, I., Gallino, R., et al. 2002, *ApJ*, 579, 817
- Abia, C., Domínguez, I., Gallino, R., et al. 2003, *PASA*, 20, 314
- Abia, C. & Isern, J. 2000, *ApJ*, 536, 438

- Alvarez, R. & Plez, B. 1998, *A&A*, 330, 1109
- Alves, D. R. 2000, *ApJ*, 539, 732
- Aoki, W., Beers, T. C., Christlieb, N., et al. 2007, *ApJ*, 655, 492
- Arenou, F., Grenon, M., & Gomez, A. 1992, *A&A*, 258, 104
- Arenou, F. & Luri, X. 1999, in *ASP Conf. Ser.*, Vol. 167, *Harmonizing Cosmic Distance Scales in a Post-HIPPARCOS Era*, ed. D. Egret & A. Heck, 13–32
- Asplund, M., Grevesse, N., & Sauval, A. J. 2005, in *ASP Conf. Ser.*, Vol. 336, *Cosmic Abundances as Records of Stellar Evolution and Nucleosynthesis*, ed. T. G. Barnes, III & F. N. Bash, 25–38
- Barbaro, G. & Dallaporta, N. 1974, *A&A*, 33, 21
- Barnbaum, C., Kastner, J. H., Morris, M., & Likkell, L. 1991, *A&A*, 251, 79
- Barnbaum, C., Stone, R. P. S., & Keenan, P. C. 1996, *ApJS*, 105, 419
- Bartkevicius, A. 1996, *Baltic Astronomy*, 5, 217
- Belczyński, K., Mikolajewska, J., Munari, U., Ivison, R. J., & Friedjung, M. 2000, *A&AS*, 146, 407
- Bergeat, J., Knapik, A., & Rutily, B. 2001, *A&A*, 369, 178
- Bergeat, J., Knapik, A., & Rutily, B. 2002a, *A&A*, 390, 967
- Bergeat, J., Knapik, A., & Rutily, B. 2002b, *A&A*, 385, 94
- Bisterzo, S., Gallino, R., Straniero, O., et al. 2006, *Mem. Soc. Astron. It.*, 77, 985
- Blanco, V. M. 1965, in *Galactic Structure*, ed. A. Blaauw & M. Schmidt
- Boothroyd, A. I. & Sackmann, I.-J. 1999, *ApJ*, 510, 232
- Busso, M., Guandalini, R., Persi, P., Corcione, L., & Ferrari-Toniolo, M. 2007, *AJ*, 133, 2310
- Caffau, E., Ludwig, H.-G., Steffen, M., et al. 2008, *A&A*, 488, 1031
- Cannon, A. J. & Pickering, E. C. 1918, *Annals of Harvard College Observatory*, 91, 1
- Cardelli, J. A., Clayton, G. C., & Mathis, J. S. 1989, *ApJ*, 345, 245
- Carquillat, J.-M. & Prieur, J.-L. 2008, *Astronomische Nachrichten*, 329, 44
- Castilho, B. V. 2000, in *IAU Symposium*, Vol. 198, *The Light Elements and their Evolution*, ed. L. da Silva, R. de Medeiros, & M. Spite, 33
- Charbonnel, C., Brown, J. A., & Wallerstein, G. 1998, *A&A*, 332, 204
- Chen, P.-S., Yang, X.-H., & Zhang, P. 2007, *AJ*, 134, 214
- Claussen, M. J., Kleinmann, S. G., Joyce, R. R., & Jura, M. 1987, *ApJS*, 65, 385
- Costa, E. & Frogel, J. A. 1996, *AJ*, 112, 2607
- Cristallo, S., Straniero, O., Gallino, R., et al. 2009, *ApJ*, 696, 797
- Cutri, R. M., Skrutskie, M. F., van Dyk, S., et al. 2003, *2MASS All Sky Catalog of point sources. (The IRSA 2MASS All-Sky Point Source Catalog, NASA/IPAC Infrared Science Archive. <http://irsa.ipac.caltech.edu/applications/Gator/>)*
- de La Reza, R. 2006, in *Chemical Abundances and Mixing in Stars in the Milky Way and its Satellites*, ed. S. Randich & L. Pasquini, *ESO ASTROPHYSICS SYMPOSIA*, 196
- de Laverny, P., Abia, C., Domínguez, I., et al. 2006, *A&A*, 446, 1107
- Dean, C. A. 1972, PhD thesis, AA(The University of Texas at Austin.)
- Dearborn, D. S. P., Lattanzio, J. C., & Eggleton, P. P. 2006, *ApJ*, 639, 405
- Denn, G. R., Luck, R. E., & Lambert, D. L. 1991, *ApJ*, 377, 657
- Despain, K. H. 1982, *ApJ*, 253, 811
- Dominy, J. F. 1984, *ApJS*, 55, 27
- Dominy, J. F., Lambert, D. L., Gehrz, R. D., & Mozurkewich, D. 1986, *AJ*, 91, 951
- Eggen, O. J. 1972, *MNRAS*, 159, 403
- Egłitis, I., Eglite, M., & Balklavs, A. 2003, *Baltic Astronomy*, 12, 353
- Elias, J. H. 1978, *AJ*, 83, 791
- Fujimoto, M. Y., Iben, I. J., & Hollowell, D. 1990, *ApJ*, 349, 580
- García-Hernández, D. A., García-Lario, P., Plez, B., et al. 2006, *Science*, 314, 1751
- Gilroy, K. K. 1989, *ApJ*, 347, 835
- Gilroy, K. K. & Brown, J. A. 1991, *ApJ*, 371, 578
- Goswami, A. 2005, *MNRAS*, 359, 531
- Guandalini, R., Busso, M., Palmerini, S., & Utenthaler, S. 2009, *PASA*, submitted
- Gustafsson, B., Edvardsson, B., Eriksson, K., et al. 2008, *A&A*, 486, 951
- Han, Z., Eggleton, P. P., Podsiadlowski, P., & Tout, C. A. 1995, *MNRAS*, 277, 1443
- Härm, R. & Schwarzschild, M. 1966, *ApJ*, 145, 496
- Hollowell, D., Iben, I. J., & Fujimoto, M. Y. 1990, *ApJ*, 351, 245
- Iben, Jr., I. & Renzini, A. 1983, *ARA&A*, 21, 271
- Ishida, K. 1960, *PASJ*, 12, 214
- Izzard, R. G., Jeffery, C. S., & Lattanzio, J. 2007, *A&A*, 470, 661
- Johnson, H. R., Eaton, J. A., Querci, F. R., Querci, M., & Baumert, J. H. 1988, *A&A*, 204, 149
- Jorissen, A. & Knapp, G. R. 1998, *A&AS*, 129, 363
- Keenan, P. C. 1993, *PASP*, 105, 905
- Keenan, P. C. & Morgan, W. W. 1941, *ApJ*, 94, 501
- Knapp, G., Pourbaix, D., & Jorissen, A. 2001, *A&A*, 371, 222
- Lambert, D. L., Gustafsson, B., Eriksson, K., & Hinkle, K. H. 1986, *ApJS*, 62, 373
- Lambert, D. L., Smith, V. V., Busso, M., Gallino, R., & Straniero, O. 1995, *ApJ*, 450, 302
- Lattanzio, J., Dearborn, D., Eggleton, P., & Dossa, D. 2006, [arXiv:astro-ph/0612147]
- Lee, O. J. & Bartlett, T. J. 1944, *Annales of the Dearborn Observatory*, 5, 67
- Lloyd Evans, T. 1986, *MNRAS*, 220, 723
- Luck, R. E. & Challener, S. L. 1995, *AJ*, 110, 2968
- Makarov, V. V. & Kaplan, G. H. 2005, *AJ*, 129, 2420
- Masseron, T., Johnson, J. A., Plez, B., et al. 2009, [arXiv:astro-ph/09014737]
- McClure, R. D. 1970, *AJ*, 75, 41
- McClure, R. D. 1997, *PASP*, 109, 256
- Mendoza, V. E. E. & Johnson, H. L. 1965, *ApJ*, 141, 161
- Mengel, J. G. & Gross, P. G. 1976, *Ap&SS*, 41, 407
- Mocák, M. 2009, PhD thesis, Max-Planck-Institut für Astrophysik, Garching bei München
- Mocák, M., Mueller, E., Weiss, A., & Kifonidis, K. 2008a, [arXiv:astro-ph/08114083]
- Mocák, M., Müller, E., Weiss, A., & Kifonidis, K. 2008b, *A&A*, 490, 265
- Morgan, W. W. & Keenan, P. C. 1973, *ARA&A*, 11, 29
- Munari, U. & Zwitter, T. 2002, *A&A*, 383, 188
- Neugebauer, G. & Leighton, R. B. 1969, *Two-micron sky survey. A preliminary catalogue (NASA SP, Washington: NASA, 1969)*
- Noguchi, K., Kawara, K., Kobayashi, Y., et al. 1981, *PASJ*, 33, 373
- Ohnaka, K. & Tsuji, T. 1996, *A&A*, 310, 933
- Paczynski, B. & Tremaine, S. D. 1977, *ApJ*, 216, 57
- Palacios, A., Charbonnel, C., & Forestini, M. 2001, *A&A*, 375, L9
- Palacios, A., Charbonnel, C., Talon, S., & Siess, L. 2006, *A&A*, 453, 261
- Perryman, M. A. C. & ESA, eds. 1997, *ESA Special Publication*, Vol. 1200, *The HIPPARCOS and TYCHO catalogues. Astrometric and photometric star catalogues derived from the ESA HIPPARCOS Space Astrometry Mission*
- Pfeiffer, M. J., Frank, C., Baumüller, D., Fuhrmann, K., & Gehren, T. 1998, *A&AS*, 130, 381
- Piersanti, L., Cabezón, R. M., Zamora, O., et al. 2009, *A&A*, in preparation
- Platais, I., Pourbaix, D., Jorissen, A., et al. 2003, *A&A*, 397, 997
- Pourbaix, D. & Jorissen, A. 2000, *A&AS*, 145, 161
- Rybski, P. M. 1972, PhD thesis, AA(Northwestern University.)
- Sanford, R. F. 1944, *Radial velocities of 283 stars of spectral classes R and N (Chicago, 1944)*, 145–161
- Scalo, J. M. 1976, *ApJ*, 206, 474
- Schild, R. E. 1973, *AJ*, 78, 37
- Schmitt, J. L. 1971, *ApJ*, 163, 75
- Schwarzschild, M. & Härm, R. 1962, *ApJ*, 136, 158
- Shane, C. D. 1928, *Lick Observatory Bulletin*, 13, 123
- Smith, V. V., Cunha, K., Jorissen, A., & Boffin, H. M. J. 1996, *A&A*, 315, 179
- Stephenson, C. B. 1973, *Publications of the Warner & Swasey Observatory*, 1
- Stock, J. & Welhau, W. H. 1956, *AJ*, 61, 80
- Straniero, O., Domínguez, I., Cristallo, R., & Gallino, R. 2003, *PASA*, 20, 389
- Totten, E. J., Irwin, M. J., & Whitelock, P. A. 2000, *MNRAS*, 314, 630
- Uppgren, A. R. 1962, *AJ*, 67, 539
- van Leeuwen, F. 2007, *A&A*, 474, 653
- van Leeuwen, F. & Evans, D. W. 1998, *A&AS*, 130, 157
- Vandervort, G. L. 1958, *AJ*, 63, 477
- Wallerstein, G. & Knapp, G. R. 1998, *ARA&A*, 36, 369
- Wallerstein, G., Kovtyukh, V. V., & Andrievsky, S. M. 2009, *ApJ*, 692, L127
- Wallerstein, G. & Sneden, C. 1982, *ApJ*, 255, 577
- Whitelock, P., Marang, F., & Feast, M. 2000, *MNRAS*, 319, 728
- Wielen, R., Dettbarn, C., Fuchs, B., Jahreiß, H., & Radons, G. 1992, in *IAU Symposium*, Vol. 149, *The Stellar Populations of Galaxies*, ed. B. Barbuy & A. Renzini, 81–92
- Yamashita, Y. 1972, *Annales de l'Observatoire astronomique de Tokyo*, 13, 167
- Yamashita, Y. 1975, *PASJ*, 27, 325
- Zamora, O. 2009, PhD thesis, *Composición química y estado evolutivo de las estrellas de carbono de tipo espectral R (Universidad de Granada, 2009, http://adrastea.ugr.es/record=b1789202*spi)*
- Začs, L., Schmidt, M. R., Musaev, F. A., Galazutdinov, G. A., & Sperauskas, J. 2005, *A&A*, 441, 303